

ChemComm

Chemical Communications

Accepted Manuscript

This article can be cited before page numbers have been issued, to do this please use: X. Yang, J. tang, D. Zhang, X. han, J. Liu, J. Li, Y. Zhao and Y. Ye, *Chem. Commun.*, 2020, DOI: 10.1039/D0CC05803C.



This is an Accepted Manuscript, which has been through the Royal Society of Chemistry peer review process and has been accepted for publication.

Accepted Manuscripts are published online shortly after acceptance, before technical editing, formatting and proof reading. Using this free service, authors can make their results available to the community, in citable form, before we publish the edited article. We will replace this Accepted Manuscript with the edited and formatted Advance Article as soon as it is available.

You can find more information about Accepted Manuscripts in the [Information for Authors](#).

Please note that technical editing may introduce minor changes to the text and/or graphics, which may alter content. The journal's standard [Terms & Conditions](#) and the [Ethical guidelines](#) still apply. In no event shall the Royal Society of Chemistry be held responsible for any errors or omissions in this Accepted Manuscript or any consequences arising from the use of any information it contains.

COMMUNICATION

An AIE probe for imaging mitochondria SO₂-induced stress and its level in heat strokeReceived 00th January 20xx,
Accepted 00th January 20xx

DOI: 10.1039/x0xx00000x

Xiaopeng Yang^a, Jun Tang^a, Di Zhang,^{*b} Xiaojing Han^a, Jianfei Liu^a, Jinsa Li^a, Yufen Zhao^{a,c}, Yong Ye^{*a}

A probe MITO-TPE was developed for imaging mitochondrial SO₂ with good selectivity, high sensitivity, and fast response. Cell imaging indicated that SO₂ induced oxidative stress may cause damage to cells through O₂^{•-} bursting. MITO-TPE has been achieved imaging the misregulation of SO₂ level in mitochondria during heat stroke for the first time.

Sulfur dioxide (SO₂), which traditionally recognized as a toxic gas or environmental pollutant, may be a new member of the growing family of gaseous signaling molecules in addition to NO, CO and H₂S¹. In biological system, SO₂ is one of the important metabolites of SH-containing amino acids such as cysteine (Cys). Additionally, SO₂ is dissociated into its two derivatives sulfite (SO₃²⁻) and bisulfite (HSO₃⁻) in humoral environment². However, excessive SO₂ is related to lung cancer, and many neurological diseases, including strokes, migraine headaches, and brain cancers³. The role of SO₂ in physiological environment has received increased attention across a number of disciplines in recent years⁴. More evidence suggests that SO₂ has corrosive and irritating effects on the respiratory mucosa, and lead to airway obstructive diseases. Researchers have attempted to explore toxicological effect of SO₂ associated with respiratory system, but ignored the damage of SO₂ to other organisms and systems in the body. After SO₂ is inhaled into the human body, various sulfur-centered radicals and oxygen-centered radicals can be formed through metabolic transformation, leading to the formation of superoxide anions radicals (O₂^{•-}). These free radicals can cause oxidative damage to the body, which may be one of the main mechanisms of SO₂-induced cytotoxicity⁵. So far, there has been agreement about the excessive inhalation of SO₂ causes peroxidation of lipids in different organs, which not only

causes severe oxidative damage to the respiratory system, but also to other organs including brain, heart, liver, kidney⁶. Therefore, it is an urgent need to develop an effective method for monitoring the SO₂-induced oxidative stress, which is very meaningful to study biological toxicity mechanism of SO₂ to the body.

Heat stroke was induced by exposing to a high ambient temperature of 40.6 °C⁷. In the case of severe heat stroke, heart rate and respiration rate will increase as blood pressure drops and the heart attempts to supply enough oxygen to the body⁸. When the body temperature is higher than 41 °C, the enzyme becomes denatured and mitochondrial dysfunction occurs⁹. The cell membrane is unstable and the oxygen-dependent metabolic pathway is destroyed. But in spite of these associations, the mitochondrial behavior during a heat shock process is still little known. Moreover, SO₂ plays an important role in oxidative stress and cell homeostasis¹⁰. It is worth studying the relationship between the mis-regulation of SO₂ level in mitochondria and temperature. Consequently, accurately monitoring the SO₂ changes in mitochondria during heat shock is essential to understanding the mechanism of heat cytotoxicity.

Owing to the advantages of simple operation, high sensitivity, low cost, and non-destructive, fluorescent probes have been widely used in biological fields such as living cells and tissues to monitor chemical substances¹¹. Because aggregation-induced emission (AIE)-based fluorescent probes could work well at high concentrations, more and more AIE molecules were used for fluorescence analysis. There will be corresponding changes in the fluorescence signal for detection of analytes which can adjust the dispersion and aggregation state of AIE molecules¹². In addition, AIE molecules also provide new strategy for designing fluorescent probes¹³. To date, lots of fluorescent probes have been developed for SO₂ derivatives detection based on aldehyde, levulinate, Michael addition and metal coordination complex¹⁴. However, a fast, sensitive and selective AIE fluorescence probe for SO₂ detection is still missing.

Herein, our group constructed a novel AIE and mitochondrion-targeted fluorescent probe (MITO-TPE) combining tetraphenylethene (TPE) and benzopyrylium as

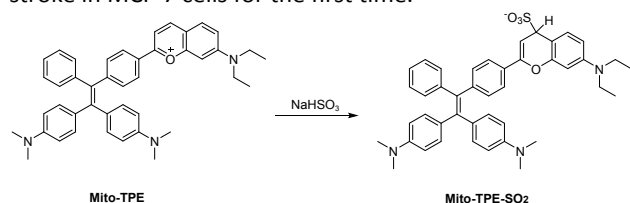
^a Green Catalysis Center, and College of Chemistry, Zhengzhou University, Zhengzhou 450001, China. E-mail: yeyong03@tsinghua.org.cn.

^b Institute of Agricultural Quality Standards and Testing Technology, Henan Academy of Agricultural Sciences, Zhengzhou 450002, China. E-mail: pandy811@163.com

^c Institute Drug Discovery Technology, Ningbo University, Ningbo 315211, Zhejiang, China

†Electronic Supplementary Information (ESI) available: Materials and methods; photophysical data; bioimaging; synthetic details, NMR and HR-MS spectra. See DOI: 10.1039/x0xx00000x

illustrated in Scheme 1. Notably, **MITO-TPE** showed strong green fluorescence after SO_2 derivatives react with C=C bonds of benzopyrylium by 1, 4-conjugate addition. Through the specific reaction with SO_2 , the probe showed ultrasensitive, highly selective and fast-responsive detection for SO_2 . In addition, **MITO-TPE** was successfully employed for imaging mitochondrial SO_2 . Cell imaging indicated that the extra SO_2 was able to modulate oxidative stress by increasing the $\text{O}_2^{\cdot -}$ levels and further cause tissues and organs damage. We found that the mis-regulation of mitochondrial SO_2 levels under heat stroke in MCF-7 cells for the first time.



Scheme 1. Proposed reaction mechanism of **MITO-TPE** with NaHSO_3 .

The fluorescent probe **MITO-TPE** was easily prepared through a few steps according to the route in Scheme S1. Intermediate **M4** was synthesized by lithiation of **M3** with *n*-Butyllithium and acetylation with dimethylacetamide. Compound **M4** reacted with 4-(Diethylamino) salicylaldehyde in concentrated sulfuric acid to give designed probe **MITO-TPE**. And the structure of probe was confirmed by HR-MS, ^1H NMR and ^{13}C NMR spectra (Figures S1-3). At first, we examined the response of **MITO-TPE** toward HSO_3^- with AIE property which has almost no fluorescence in distinct polar solvents, but have strong fluorescence in polar solvents or solid states. We used compound **MITO-TPE-SO₂** (an analog of the reaction product of the probe molecule with HSO_3^-) for verification. As shown in Figure S4, **MITO-TPE-SO₂** showed negligible fluorescence in the pure DMSO solution. However, fluorescence intensity of the **MITO-TPE-SO₂** gradually increased with the enhancement of water ratio. The fluorescent intensity of **MITO-TPE-SO₂** in 99% water solution was 15 times higher than that in pure DMSO. The results demonstrate that **MITO-TPE-SO₂** is a fluorescent material with AIE property.

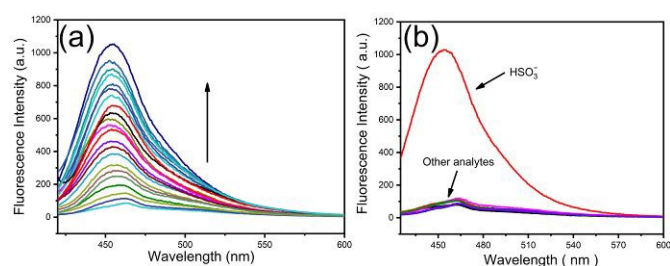


Figure 1. (a) Fluorescence emission spectra of **MITO-TPE** ($10.0 \mu\text{M}$) upon the addition of increasing concentrations NaHSO_3 ($0 - 100 \mu\text{M}$). (b) The selectivity of **MITO-TPE** ($10 \mu\text{M}$) to NaHSO_3 ($100 \mu\text{M}$) and $100 \mu\text{M}$ other various relevant species (F^- , Cl^- , Br^- , I^- , AcO^- , HCO_3^- , CO_3^{2-} , GSH , Hcy , Cys , NO_3^- , NO_2^- , NO , HNO , ONOO^- , O_2^- , H_2O_2 , ClO^- , TBHP , $\cdot\text{OH}$, $^1\text{O}_2$, S^{2-} , HS^- , SO_4^{2-} , $\text{S}_2\text{O}_3^{2-}$, PO_4^{3-} , N_3^- , SCN^-) in the PBS buffer (10 mM , $\text{pH}=7.4$).

Then, we studied the sensing ability of probe **MITO-TPE** towards HSO_3^- in PBS buffer (10 mM , $\text{pH} 7.4$). **MITO-TPE** ($10 \mu\text{M}$) exhibited a strong absorption at 490 nm . The benzopyrylium absorption band at 490 nm markedly decreased upon the addition of HSO_3^- (Figure S5). We first

tested the fluorescence change of the probe under excitation at 490 nm , and the probe **MITO-TPE** showed negligible fluorescence emission (Figure S6). When HSO_3^- was added, the fluorescence decreased slightly. We then checked the fluorescence of free **MITO-TPE** under excitation at 400 nm (Figure 1a) and a weak fluorescence emission at 455 nm was observed. With the increasing of concentration of HSO_3^- , the fluorescence emission at 455 nm gradually enhanced. It is known to all that the content of SO_2 derivatives in the human body is low, so the detection limit of the probe is an important indicator to determine whether the probe can be used in a physiological environment. The fluorescence intensity at 455 nm was linearly related to the concentration of HSO_3^- (Figure S7) with a good linear relationship ($R^2=0.9884$). The detection limit was calculated to be $27.22 \mu\text{M}$ ($\text{DL}=3\sigma/k$) which indicated that probe **MITO-TPE** is highly sensitive to HSO_3^- and exhibited the potential use for quantitative determination of HSO_3^- . The response of the probe toward HSO_3^- was fast (Figure S8). The maximum plateau was reached within 20 s . To the contrary, the emission of probe **MITO-TPE** exhibited almost negligible changes indicating that the probe was stable in PBS solution.

Next, we examined the selectivity of **MITO-TPE** to HSO_3^- . As shown in Figure S9, the probe **MITO-TPE** ($10 \mu\text{M}$) exhibited central absorption at 490 nm . No significantly change in the max absorption was observed upon the addition of different biologically relevant molecules except HSO_3^- . In addition, only introduction of HSO_3^- to the **MITO-TPE** solution could trigger the fluorescence emission at 455 nm significantly enhanced (Figure 1b). The addition of 10 equiv other biologically relevant molecules did not induce any changes in the fluorescence emission. Moreover, it is also worth noting that even in the presence of other analytes shown in Figure S10, probe **MITO-TPE** still could specifically respond toward HSO_3^- . Clearly, those results demonstrated that probe **MITO-TPE** performed excellent selectivity and potential applications for detection of HSO_3^- without any distinct interference from other biologically relevant species in complex biological environments.

In order to investigate whether **MITO-TPE** can meet the original design purpose of detecting SO_2 derivatives, the fluorescence emission spectra of probe **MITO-TPE** in different pH environments were tested in the absence or presence of HSO_3^- (Figure S11). The maximal emission intensity was observed with pH ranging $6-11$. In addition, we studied the fluorescence emission of probe **MITO-TPE** ($10 \mu\text{M}$) in different temperature environments in the absence or presence of HSO_3^- (Figure S12). The probe alone showed weak emission, and the fluorescence emission at 455 nm significantly enhanced after the addition of HSO_3^- ($0-100 \mu\text{M}$). Those results indicated that the probe could be applied for SO_2 derivatives imaging in physiological environment as designed.

To explore the addition reaction mechanism of probe **MITO-TPE** depicted in Scheme 1, HR-MS was used to analyze the process of the reaction between **MITO-TPE** and HSO_3^- . The mass spectral analysis of probe treated with HSO_3^- displayed a new peak at $m/z 698.3073$ corresponded to the addition product **MITO-TPE-SO₂** ($\text{C}_{43}\text{H}_{44}\text{N}_3\text{O}_4\text{S}$) (Figure S13). These results demonstrated that the HSO_3^- was reacted with C=C of

benzopyrylium via Michael addition, the conjugate structure was effectively blocked, which lead to the probe **MITO-TPE** favourable for the SO_2 derivatives imaging.

In order to investigate whether the probe **MITO-TPE** has good bioavailability, the cytotoxicity of the probe **MITO-TPE** was evaluated. First, the MCF-7 cell suspension was dropped on a 96-well culture plate, and then cultured in a cell incubator at 37 °C and 5% CO_2 for 24 h. **MITO-TPE** solutions of different concentrations (0, 5, 10, 15, 20 μM) were added, and the cells were cultured in the cell incubator for 24 h. Then, CCK8 (10 μL) was added and incubated for 2 h. The absorbance at 450 nm was determined with enzyme-labelled instrument. As shown in Figure S14, the experimental data showed that the cell viability is still around 90% after treated with 20 μM probe **MITO-TPE**. The experimental results illustrated that the toxicity of the probe is basically negligible to cells.

We further investigated the application of probe for SO_3^{2-} imaging in living cells. In the beginning, MCF-7 cells were pretreated with the probe **MITO-TPE** (10 μM) solution for 0.5 h, and imaged by confocal fluorescence microscope after washing three times with PBS buffer solution, displayed weak fluorescence emission as illustrated in Figure S15a. In contrast, probe-pretreated cells were incubation with exogenous 100 μM SO_3^{2-} for another 0.5 h, the imaging of cell showed strong fluorescence (Figure S15b). FA (formaldehyde), known as a bisulfite inhibitor, was used to clear the bisulfite in the cell¹⁰. The probe-pretreated cells with 100 μM SO_3^{2-} were treated 200 μM FA for 0.5 h, the cells showed negligible fluorescence (Figure S15c). Time-dependent confocal images of **MITO-TPE** toward SO_2 was investigated. Upon the addition of Na_2SO_3 , the fluorescence intensity of cells increased in a short period time (Figure S16). Taken together, those results demonstrated that the probe can effectively imaging SO_2 derivatives with good biocompatibility and membrane permeability in the cell.

To further investigate the probe **MITO-TPE** can be used for mitochondria SO_2 detection, we conducted co-localization experiment in MCF-7 cells. The cells were incubated probe **MITO-TPE** (10 μM) and commercial mitochondria indicator Mito-Tracker Red (100 nM) for 0.5 h. Then MCF-7 cells continue to be incubated upon the addition of another 100 μM Na_2SO_3 for 0.5 h. Cell imaging studies were taken on confocal fluorescence microscopy after washed three times with PBS buffer solution as illustrated in Figure S17. The probe **MITO-TPE** showed obviously green fluorescence emission in channel 1 (Figure S17a). Meanwhile, the Mito-Tracker Red also displayed strong red fluorescence emission in channel 2 (Figure S17b). The overlay image demonstrated that the fluorescence emission of probe **MITO-TPE** and Mito-Tracker Red overlapped well (Figure S17c). The Pearson coefficient and overlap coefficient are 0.9147 and 0.9032, respectively. Co-localization experiments indicated that probe **MITO-TPE** can specifically located to mitochondria with the potential for real-time imaging mitochondria SO_2 derivatives in vivo.

SO_2 -induced oxidative stress may be one of the mechanisms to cause damage to cells. Monitoring oxidative stress caused by SO_2 in cells which still faces great challenge. $\text{O}_2^{\cdot-}$ is one of the markers of oxidative stress, and hydroethidium (**HE**)¹⁵ has

been proved that can freely enter the cell and dehydrogenate to form ethidium bromide under the oxidation of intracellular $\text{O}_2^{\cdot-}$ (Scheme S2). Here, we had successfully applied probe **MITO-TPE** to real time image the SO_2 -induced oxidative stress process under the red channel. As shown in Figure 2a, cells showed almost no fluorescence in green and red channel upon treatment with probe **MITO-TPE** and **HE** (10 μM). After the MCF-7 cells were pretreated with 500 μM Na_2SO_3 for 2 h, then cells were stained with probe **MITO-TPE** and **HE** (10 μM) for another 0.5 h. The fluorescence was simultaneously enhanced in green and red channel (Figure 2b). This illustrated that SO_2 induced the production of $\text{O}_2^{\cdot-}$. As Figure 2c shown, the cells were first treated with N-acetyl-L-cysteine (NAC) 1 mM for 1 h, then added with 500 μM Na_2SO_3 and incubated for 2 h. When the cells were further treated with probe **MITO-TPE** and **HE** (10 μM), the fluorescence of the green channel exhibited significantly enhancement, while the fluorescence of the red channel showed a negligible change. The results showed that NAC can effectively inhibit the production of $\text{O}_2^{\cdot-}$ caused by SO_2 . In addition, SO_2 -induced oxidative stress may cause damage to cells through $\text{O}_2^{\cdot-}$ bursting.

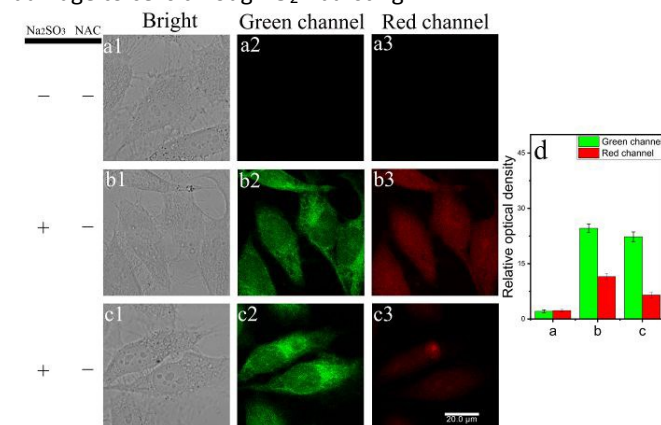


Figure 2. Fluorescence images of SO_2 -induced oxidative stress in MCF-7 cells. (a) cells treated with probe **MITO-TPE** (10 μM) and **HE**(10 μM). (b) cells incubated with Na_2SO_3 (500 μM) then treated with probe **MITO-TPE** (10 μM) and **HE** (10 μM). (c) NAC-pretreated (1 mM) cells incubated with Na_2SO_3 (100 μM) and then treated with **MITO-TPE** (10 μM) and **HE** (10 μM). (d) Relative optical density of the respect wells. (Chanel 1: λ_{ex} = 405 nm, emission: 425-485 nm, Chanel 2: λ_{ex} = 488 nm, emission: 575-635 nm, Scale bar: 20 μm).

Heat stroke response is an important cytoprotective process in regulating cell homeostasis against not only environmental stresses (e.g. temperature, ROS and pathogens infection), but also the intracellular stresses (cell proliferation and differentiation). So, we studied SO_2 and $\text{O}_2^{\cdot-}$ concentration changes under heat stroke in MCF-7 cells. Cells were first treated with **MITO-TPE** (10 μM) for 0.5 h at 37 °C. Next, the cells were placed at 37, 39, 41, 43 and 45 °C and incubated for 1 h. As shown in Figure 3a, there is almost no fluorescence in the cells under the incubation condition at 37 °C. Weak fluorescence can be observed in the cell under the incubation condition at 39 and 41 °C (Figure 3b, c). Under the incubation condition of 43 and 45 °C, obvious fluorescence can be observed (Figure 3d, e). The results indicate that the

generation of SO_2 is related to the cell culture temperature. In a control experiment, FA was used to inhibit the production of SO_2 in heat shock. Pretreated of MCF-7 cells with **MITO-TPE** were incubated with FA (200 μM) for 0.5 h at 37 $^\circ\text{C}$, and then incubated at 45 $^\circ\text{C}$ for another 1 h. Unsurprisingly, cells showed negligible fluorescence emission under the presence of FA. The results indicate that the level of SO_2 increase along with cell temperature increasing, and there is a direct relationship between cell temperature and SO_2 concentration in mitochondria. More importantly, we have successfully monitored the $\text{O}_2^{\cdot-}$ burst with the increase of temperature (37 - 45 $^\circ\text{C}$) as shown in Figure S18. The level of $\text{O}_2^{\cdot-}$ increased during heat shock. Above results suggested that up-regulation of SO_2 in the mitochondria may be dependent on the oxidative stress induced by heat shock.

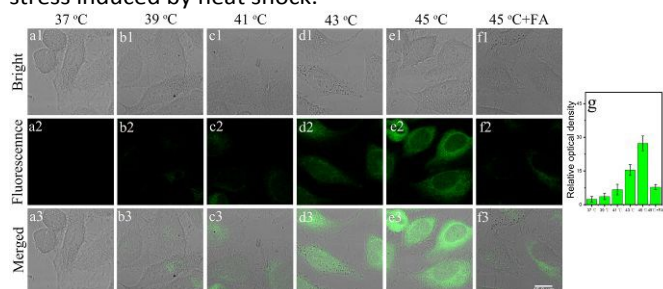


Figure 3. Fluorescence images of MCF-7 cells (a-f) incubated with **MITO-TPE** (10 μM) at different temperatures (37, 39, 41, 43 and 45 $^\circ\text{C}$). (g) Relative optical density of the respect wells. (λ_{ex} = 405 nm, emission: 425-485 nm, Scale bar: 15 μm).

As a very good vertebrate model, zebrafish is of great significance for biological imaging. The zebrafish first incubated with **MITO-TPE** (10 μM) for 0.5 h, and then used for fluorescence imaging. No fluorescence was found (Figure S19a). Zebrafish was pretreated with **MITO-TPE** (10 μM) for 0.5 h, and then 100 μM Na_2SO_3 was added to incubate for another 0.5 h. There was obvious fluorescence enhancement (Figure S19b). Further, on the basis of the previous step, 200 μM FA was added to incubate for 1 h to clear SO_2 , and weak fluorescence enhancement was found (Figure S19c). It shows that the probe also has a good imaging results for monitoring SO_2 in zebrafish.

In summary, we rational designed a new fluorescent probe **MITO-TPE** for monitoring mitochondrial SO_2 based on AIE with the advantages of novel structure, good selectivity, high sensitivity and fast response. The probe realized the imaging of SO_2 in mitochondria of MCF-7 cells. In addition, we firstly reported imaging the $\text{O}_2^{\cdot-}$ caused by SO_2 -induced oxidative stress in mitochondria. The results indicated that oxidative stress is closely related to the pathogenic mechanism of excessive SO_2 . Furthermore, **MITO-TPE** was applied to monitor SO_2 produced in mitochondria during heat stroke for the first time. We believe that **MITO-TPE** provides an effective analysis

tool for deeply understanding pathogenic mechanism of excessive SO_2 and mis-regulation of SO_2 levels in heat stroke.

This work was financially supported by the NSFC (21907025), Scientific and Technological Project of Henan Province of China (192102310140), and Scientific and Technological Innovation Project of Henan Academy of Agricultural Sciences (2020CX05).

Conflicts of interest

There are no conflicts to declare.

Notes and references

- X.-B. Wang, J.-B. Du and H. Cui, *Life Sci.*, 2014, **98**, 63-67.
- Z. Meng, *Inhal. Toxicol.*, 2003, **15**, 181-195.
- X.-L. Huang, Y. Liu, J.-L. Zhou, Y.-C. Qin, X.-B. Ren, X.-H. Zhou and H. Cao, *Coord. Chem. Rev.*, 2013, **27**, 389-397.
- (a) K. Li, L.-L. Li, Q. Zhou, K.-K. Yu, J. S. Kim and X.-Q. Yu, *Coord. Chem. Rev.*, 2019, **388**, 310-333; (b) W. Wang and B. Wang, *Front. Chem.*, 2018, **6**, 189.
- H. Niu, J. Tang, X. Zhu, Z. Li, Y. Zhang, Y. Ye and Y. Zhao, *Chem. Commun.*, 2020, **56**, 7710-7713
- Y. Yan, L. Zhang, Q. Wu, Z. Chen, C. Yang, J. Zhang, M. Yu, M. Hong and J. Zhao, *Sci. China Chem.*, 2015, **45**, 1145-1158.
- Y. Wen, W. Zhang, T. Liu, F. Huo and C. Yin, *Anal. Chem.*, 2017, **89**, 11869-11874.
- S.-L. Shen, X.-F. Zhang, Y.-Q. Ge, Y. Zhu, X.-Q. Lang and X.-Q. Cao, *Sensors Actuators B: Chem.*, 2018, **256**, 261-267.
- L. Zeng, J. Tan, W. Lu, T. Lu and Z. Hu, *Cell. Signal.*, 2013, **25**, 2312-2319.
- (a) W. Zhang, Y. Yongkang, Y. Zhang, J.-B. Chao, F. Cheng and C. Yin, *J. Am. Chem. Soc.*, 2020, **142**, 3262-3268. (b) W. Zhang, F. Huo and C. Yin, *Org. Lett.*, 2019, **21**, 5277-5280.
- (a) H.-B. Cheng, Y. Li, B. Z. Tang and J. Yoon, *Chem. Soc. Rev.*, 2020, **49**, 21-31; (b) H. Li, W. Shi, X. Li, Y. Hu, Y. Fang and H. Ma, *J. Am. Chem. Soc.*, 2019, **141**, 18301-18307. (c) W. Zhang, F. Huo, F. Cheng and C. Yin, *J. Am. Chem. Soc.*, 2020, **142**, 6324-6331. (d) L. Tang, P. He, X. Yan, J. Sun, K. Zhong, S. Hou and Y. Bian, *Sensors Actuators B: Chem.*, 2017, **247**, 421-427.
- J. Wang, C. Li, Q. Chen, H. Li, L. Zhou, X. Jiang, M. Shi, P. Zhang, G. Jiang and B. Z. Tang, *Anal. Chem.*, 2019, **91**, 9388-9392.
- (a) J. Shi, Q. Deng, C. Wan, M. Zheng, F. Huang and B. Tang, *Chem. Sci.*, 2017, **8**, 6188-6195; (b) C. W. T. Leung, Y. Hong, S. Chen, E. Zhao, J. W. Y. Lam and B. Z. Tang, *J. Am. Chem. Soc.*, 2013, **135**, 62-65; (c) W. Fu, C. Yan, Z. Guo, J. Zhang, H. Zhang, H. Tian and W.-H. Zhu, *J. Am. Chem. Soc.*, 2019, **141**, 3171-3177; (d) T. Zang, Y. Xie, S. Su, F. Liu, Q. Chen, J. Jing, R. Zhang, G. Niu and X. Zhang, *Angew. Chem. Int. Ed.*, 2020, **59**, 10003-10007.
- Y. Yue, F. Huo, P. Ning, Y. Zhang, J. Chao, X. Meng and C. Yin, *J. Am. Chem. Soc.*, 2017, **139**, 3181-3185.
- X. Gao, C. Ding, A. Zhu and Y. Tian, *Anal. Chem.*, 2014, **86**, 7071-7078.